



Short communication

180 Ah kg⁻¹ specific capacity positive tubular electrodes for lead acid batteries

J. de Andrade*, P.R. Impinnisi, D.L. do Vale

Institute of Technology for Development, LACTEC, P.O. Box 19067, Curitiba, PR, Brazil

ARTICLE INFO

Article history:

Received 30 June 2010

Received in revised form 30 August 2010

Accepted 31 August 2010

Available online 6 September 2010

Keywords:

Nanometric positive active material

Tubular electrode

Lead acid battery

ABSTRACT

Two disadvantages of lead acid batteries are poor power and energy densities and the necessity of relatively long recharging times. In this paper it is presented the results of ongoing work aimed at increasing both the positive active material (PAM) specific capacity and the positive plate charge acceptability.

The experimental results show that adequate curing processes can be used to develop an interconnected structure among nanometric PbO₂ particles to produce tubular electrodes with specific capacity higher than 180 Ah kg⁻¹ and maintain this value for 130 cycles with deep discharges.

These PbO₂ positive plates are expected to exhibit higher charge acceptability due to their larger PAM surface area as compared to conventional ones, but the results indicate that the high internal ohmic resistance of the grid/PAM zone limits the fast charge efficiency.

© 2010 Elsevier B.V. All rights reserved.

1. Introduction

Lead acid battery tubular plates are usually assembled from a mixture of PbO and Pb₃O₄. The typical specific capacity for the plates is approximately 120 Ah kg⁻¹ [1], and their microstructure consists of micrometric particles with 2 m² g⁻¹ surface area [2]. The transformation of the material during the curing/formation processes is responsible for the structural integrity and electrical contact among the active material particles. Tubular electrodes assembled directly with PbO₂ particles are able to provide satisfactory discharge capacity if mounted with high enough density, to ensure a minimal pressure among the particles. Tubular plates mounted with 3.8 g cm⁻³ of PbO₂ extracted from a commercial pasted plate were found to furnish up to 80 Ah kg⁻¹ [3]. Bervas et al., using nanometric PbO₂ synthesised by oxidation of Pb²⁺ ions with ammonium persulphate in an alkaline media, were able to construct tubular electrodes with 100 Ah kg⁻¹, which were capable of withstanding more than 150 charge/discharge cycles in 2 M sulphuric acid [4]. The utilisation coefficient and power output capability of tubular electrodes can be improved by adjusting the geometry of the components and the charge regimen. Pavlov and co-workers [5–7] had shown that tubular plates with strap grids current collectors (*Strap Grid Tubular Plates*, STGP) and thinner PAM layer can furnish up to 140 Ah kg⁻¹ (C₂₀) specific capacity, can present high enough output power to meet the requirement for EV's and HEV's application, and also can withstand more than 1000 EV cycles which means more than 50,000 km.

The influence of the active material thickness on the utilisation coefficient was already reported by Faber back in the 1970s [8]. Faber had shown that the smaller the PAM thickness, the greater its utilisation coefficient for conventional geometry tubular electrodes and also for Ti fibre electrodes.

Still, when considering batteries for EV's and PHEV's, the susceptibility to fast charge is a highly desirable feature. However it is commonly associated with a high rate of heat generation and high overvoltage, which are both potentially hazardous for lead acid batteries.

Different physicochemical processes control the plate polarization that depends on the plate characteristics and the battery usage protocol. One method to decrease the plate overpotential during charging is to use active material particles with high area to volume ratios. This would decrease the actual current density during charging and, consequently, the reaction zone polarization. This reasoning leads to the conclusion that positive plates with nanometric active materials should have a higher susceptibility to fast charging than conventional plates.

Recent work has reported methods to synthesise nanometric PbO₂ particles [4,9], which could be beneficial to lead acid battery technology due to their presumable large surface area.

From the agglomerate of spheres model [10] for positive active material (PAM) particles, it can be concluded that the first necessity of any methodology to produce positive electrodes is to build up the necks between the particles and the contacts between the particles and the spine.

2. Experimental

The nanometric PbO₂ was synthesised from the hydrolysis of lead (IV) acetate, according to the method used by Caballero et

* Corresponding author. Tel.: +55 41 3361 6164; fax: +55 41 3361 6163.

E-mail addresses: juliano2@lactec.org.br (J. de Andrade), rodolfo@lactec.org.br (P.R. Impinnisi), daniela.vale@lactec.org.br (D.L. do Vale).

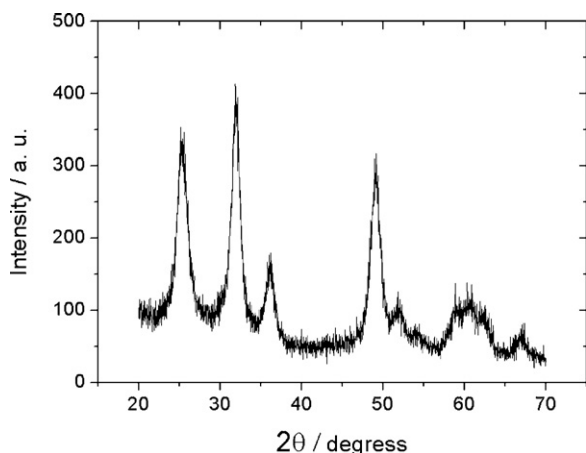


Fig. 1. Diffractogram of the nanometric PbO₂.

al. [9]. Fig. 1 shows the diffractogram of the synthesised material.

The pattern corresponds to that of β-PbO₂ [11]. Using the Scherrer equation and the parameters of the highest peak, the mean diameter of the particles was estimated to be approximately 10 nm [12]. Fig. 2 shows a TEM image of the synthesised material, confirming the mean diameter estimate.

The surface (BET) area, measured using N₂ adsorption, was 32 m² g⁻¹.

Fig. 3 shows a schematic representation of the electrodes.

The amount of PbO₂ in each electrode was 1.5 g ($\rho \sim 3.5 \text{ g cm}^{-3}$).

Different methods to build up the interconnected structure of the PbO₂ electrode have been tested on the basis of the following criteria: (a) the utilisation coefficient of the positive active material and (b) the residual capacity after removal of the tubular gauntlet. Only the results of the utilisation coefficient measurements obtained with the best curing process will be shown for comparison. Details of the different methods have been shown in Ref. [13]. The electrode susceptibility to fast charging was

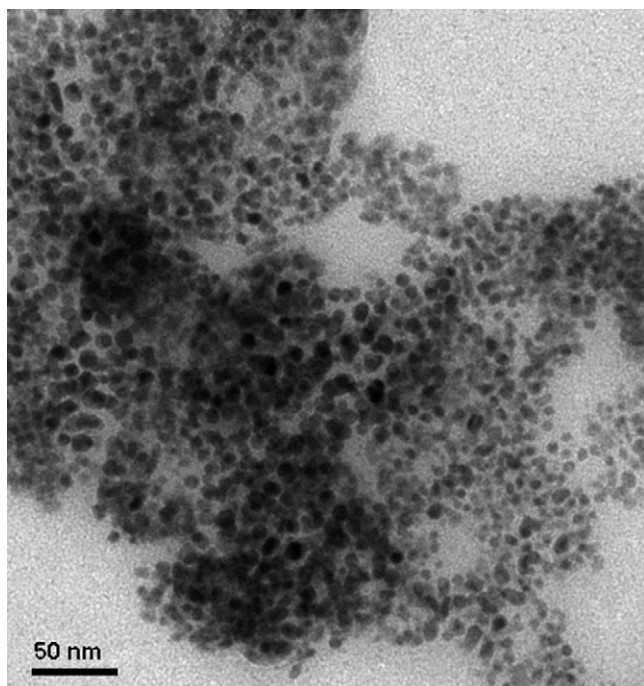


Fig. 2. TEM image of the synthesised PbO₂ particles.

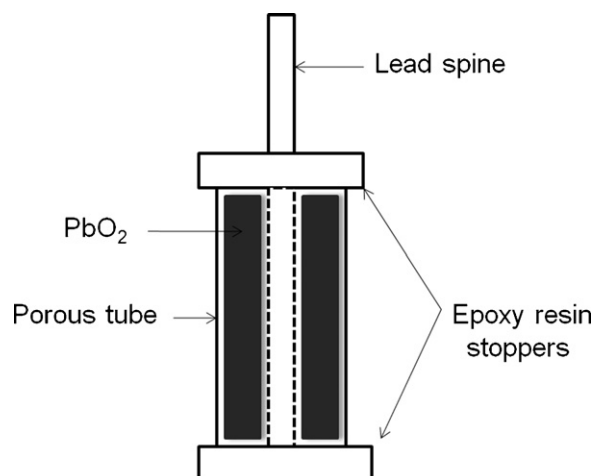


Fig. 3. A schematic representation of the tubular electrodes. The porous tube had a height of 20 mm and an internal diameter of 8.6 mm. The lead spine had a diameter of 3 mm.

also evaluated using pulsed charge algorithms. All electrochemical measurements were conducted in standard three-electrode electrochemical cells. The potential values were measured with Hg/Hg₂SO₄/H₂SO₄ reference electrodes with the acid solution having the same concentration as the cell.

3. Results

3.1. Utilisation coefficient measurements

A typical potential versus time discharge curve for a nano PbO₂ electrode in 2 M sulphuric acid solution can be seen in Fig. 4.

No significant difference can be found between the discharge curve show in Fig. 4 and one of a typical tubular electrode [14].

The discharges for utilisation coefficient measurements was performed down to 0.75 V cut off potential, in a 30 h regimen and the charge factor was 1.3.

Fig. 5 shows the specific capacity evolution of a typical electrode, which was prepared and submitted to discharge/charge cycles without any curing process. The current densities were $i_{\text{charge}} = 10 \text{ mA g}^{-1}$ and $i_{\text{discharge}} = 5 \text{ mA g}^{-1}$.

As shown in Fig. 5, the electrode assembled with nanostructured PbO₂ and without curing process performed poorly with a utilisation coefficient less than the typical values for regular tubular

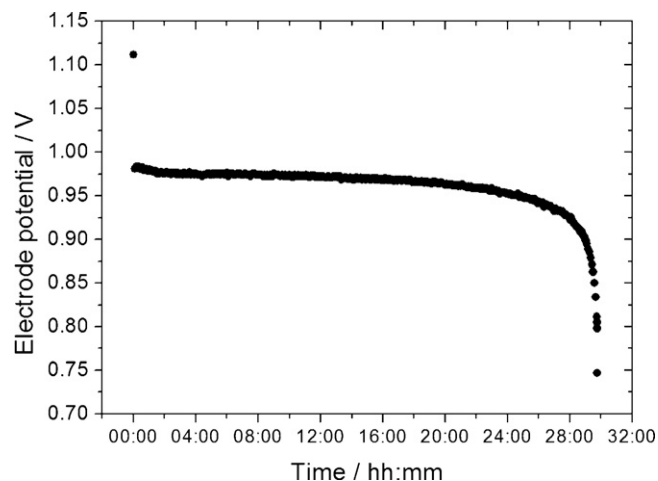


Fig. 4. Typical discharge curve at 30 h rate for a nanometric PbO₂ tubular electrode.

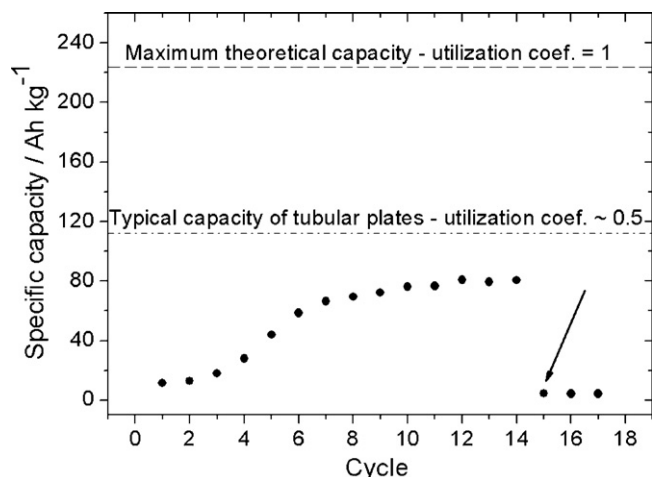


Fig. 5. Discharge capacity during charge/discharge cycles for an electrode assembled with PbO_2 nanostructures and without curing process. At the data point marked by the arrow, the experiment was stopped, the electrode tube was carefully removed and the cycles were re-started.

plates but in agreement with previous reports for tubular electrodes assembled directly with PbO_2 [3]. The capacity increased during the first cycles, indicating that some contact between the particles had been established. But after removing the gauntlet (indicated by an arrow), the electrode fell apart almost completely.

The performance of an electrode submitted to the curing process and under the same experimental conditions as the electrode in Fig. 5 is shown in Fig. 6.

Prior to the measurements, the electrode was incubated for two hours in 2 M sulphuric acid solution, washed with deionised water, dried, replaced into the electrochemical cell and submitted to an anodic current of 5.0 mA g^{-1} for 30 min. The stabilised capacity value was very high and remained high after removing the gauntlet, indicating that the pretreatment and the first charge/discharge cycle built up the interparticle necks to produce an aggregated structure. The specific capacity determined after the tubular holder removal accounted for the amount of active mass lost during the dismounting processes, which was about 7%.

The pretreatment did not significantly increase the average diameter of the nanometric PAM particles. After the pretreatment and 20 charge/discharge cycles, the PAM particles size was approx-

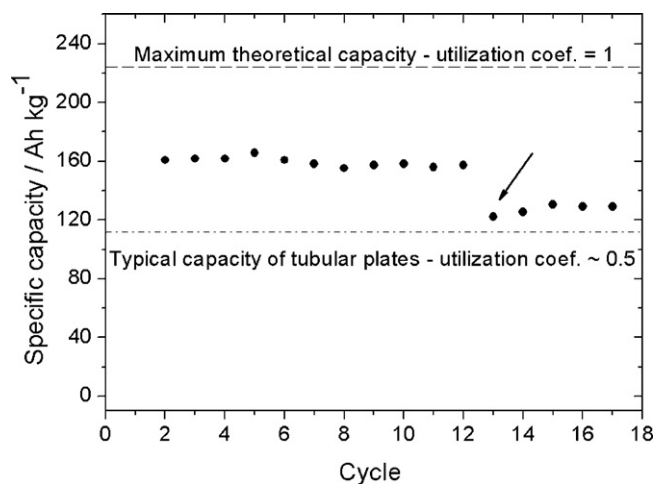


Fig. 6. Specific capacity versus cycle number for an electrode submitted to 2h immersion in 2 M sulphuric acid solution, washed, dried, placed into the electrochemical cell and galvanostatically oxidised before the cycles.

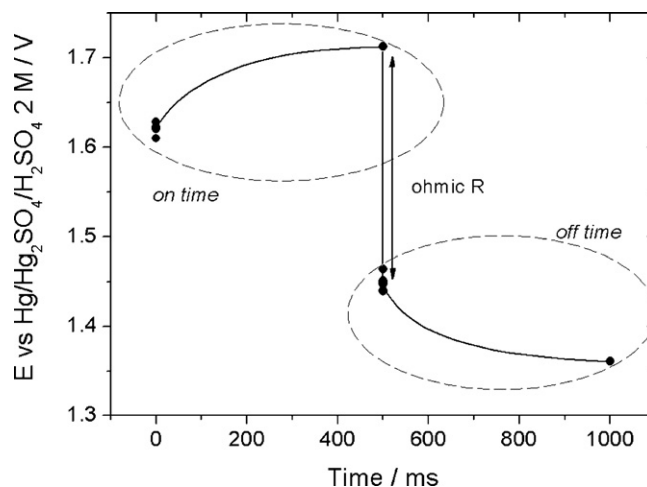


Fig. 7. The electric potential variation of a nanometric PbO_2 electrode during a single charge pulse.

imately 20 nm, and its specific surface area decreased only to $20 \text{ m}^2 \text{ g}^{-1}$.

3.2. Susceptibility to fast charge

The nanometric PbO_2 tubular electrodes were tested using charge/discharge cycles with pulsed fast charges and its behaviour was compared to tubular plates made of PbO .

The tubular PbO electrodes were mounted according to Ref. [15] because of their known high specific capacity value.

The efficiency of the pulsed charge was measured on both plates. The parameters for the charge algorithm consisted of a 1 Hz frequency, which was found to be the optimum value [16,17], a 50% duty cycle and a $2C_{30}$ current. This charging protocol would be expected to completely charge the electrode in 1 h if no side reactions occur.

The electrodes were charged using a charge factor of 1. The measured capacity is the amount of charge “absorbed” by the electrode. The efficiency of the charge regimen is defined as the ratio between the measured capacity and the nominal capacity of the electrode.

The pulsed charge applied to electrode A in which only PbO was used as precursor material, and it had an efficiency of 65%. For electrode B, made with nanometric PbO_2 , the pulsed charge efficiency was only 40%. It was expected that the nanometric PbO_2 electrodes would result in a higher charge acceptance due to their larger surface area. An analysis of the potential curve trough charge explains this behaviour, but it is first necessary to consider some basic aspects of the potential versus time curve in a single pulse.

Fig. 7 shows how the potential of a PbO_2 electrode behaves during a single charge pulse. The period with current flow is called *on time* (t_{on}), and *off time* (t_{off}) is the rest period.

The abrupt variation in the potential value during the transition from t_{on} to t_{off} is caused by the ohmic component of the total system resistance. It is attributed to the electrode external contacts, the cables, the lead spine and the active material particles. The potential variations during the on and off times (the regions marked by ellipses in Fig. 7) are attributed to ion diffusion phenomena.

The evolution of the plate potential during an entire pulse charge can provide information about the variation of its ohmic resistance. However, if the complete curve with all the data points were plotted, the resulting graph would be a miscellany of curves that would compromise a clear observation. To display the ohmic variation of the plate potential during the pulse charge experiments shown in Fig. 8, only the electrode potentials for the last value of *on time* and the first point of *off time* for each pulse for both PbO and PbO_2 plates

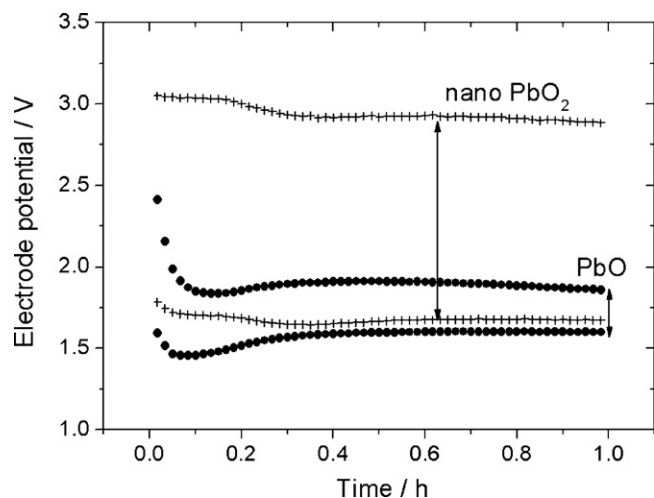


Fig. 8. Potential versus time curves during pulsed charge experiments for nanometric PbO_2 (+) and conventional PbO (●) electrodes. The arrows indicate the ohmic variation of the potential.

were plotted (the points refer to those at both ends of the arrow in Fig. 7).

The ohmic resistance for the nanometric PbO_2 electrode is higher than the PbO electrode for the entirety of the charge cycle.

The positive active material of lead acid batteries is considered to be a network of interconnected particles, i.e., the agglomerate of spheres model [10]. The total electrical and mechanical resistance is determined by the contact zone between particles or necks [18].

These considerations lead to the conflicting conclusion that, despite the high specific capacity, the nanometric PbO_2 electrode has a weak mechanical structure due to its poor conductivity. The electric current generated on the PAM (with a typical area of $3\text{--}7\text{ m}^2\text{ g}^{-1}$ and in the present work, $20\text{--}30\text{ m}^2\text{ g}^{-1}$) must flow through the spines with a typical area several orders of magnitude smaller than the PAM. A bottleneck occurs at the PAM spine interface, which determines the overall electrical resistance of the electrode, this interface encompasses the “active mass collecting layer” and the “corrosion layer” [5]. Considering this, the hypothesis of a well interconnected structure developed during the curing process remains consistent so far. If the electrode's high resistance is mainly due to the grid/PAM interface instead of the nanometric interconnections, a decrease in the PAM mass to spine surface area ratio, defined as the γ factor by Pavlov [5], would be expected to significantly decrease the ohmic polarization shown in Fig. 8.

To evaluate this prediction, an electrode assembled with nanometric PbO_2 and a 6 mm diameter spine was submitted to a pulsed charge experiment. The results are shown in Fig. 9.

Fig. 9 shows that the overpotential during the entire charge is lower for the electrode with the thicker spine, indicating that the high resistance of the plate is most likely due to the interface grid/PAM and that the pretreatment successfully formed the interconnected structure.

The efficiency of the pulsed charge for the electrode with thicker spine was higher than the thinner one, 68% versus 40%, respectively.

During the pulsed current cycles, the utilisation coefficient increased (Fig. 10).

Because of the low efficiency of the pulsed charge, each cycle shown in Fig. 10 is actually composed of two subcycles. The first subcycle was a single discharge/pulsed charge cycle that was used to evaluate the efficiency, and the second subcycle consisted of a constant current (CC) charge for 20 h to effectively measure the full capacity of the electrode.

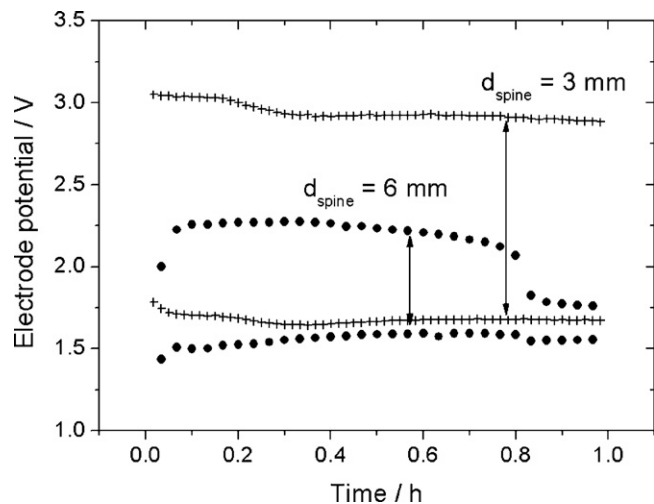


Fig. 9. Potential versus time curves during pulsed charge experiments for nanometric PbO_2 electrodes with a central spine of 3 mm diameter (+), and 6 mm diameter (●). The arrows indicate the ohmic variation of the potential.

Fig. 10 shows the evolution of the specific capacity for an electrode with a 6 mm diameter spine measured after a CC slow charge. The first six cycles were performed using only conventional charge, identical to that shown in Fig. 6, and the specific capacity value stabilised at approximately 170 Ah kg^{-1} , which was higher than the stabilised value for the 3 mm spine electrodes in Fig. 6. The next set of cycles was conducted with pulsed charges, and the specific capacity of the PAM increased to 195 Ah kg^{-1} . The same behaviour was observed for the electrodes with the thinner 3 mm spines (Fig. 11).

The specific capacities increased from 160 Ah kg^{-1} (Fig. 6) to 180 Ah kg^{-1} after the pulsed charge cycles. Considering that each cycle shown in Fig. 10 is actually composed of two deep discharges, the nanometric PbO_2 tubular electrodes endured more than a 130 deep discharges.

The explanation for this increase in the PAM utilisation coefficient is as follows: as shown by Hollekamp et al., the capacity of electrodes with pure lead grids and $\text{Pb}\text{--}\text{Ca}$ are limited by the electrical conductivity of the grid/PAM interface due to the formation of low valence lead oxides with poor electrical conductivity in this region [19]. These low valence lead oxides are oxidised to highly conductive lead oxides during the high potential period of the pulsed charges (the high potential is due to the ohmic polar-

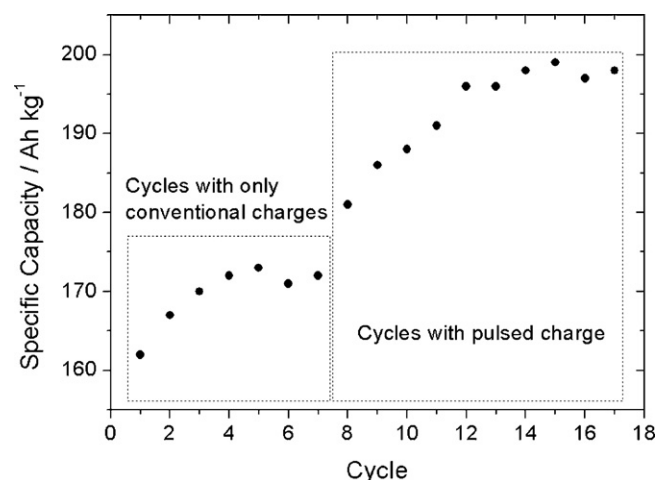


Fig. 10. Evolution of the specific capacity of the nanometric PbO_2 tubular electrode with a 6 mm diameter spine during conventional and pulsed charge cycles.

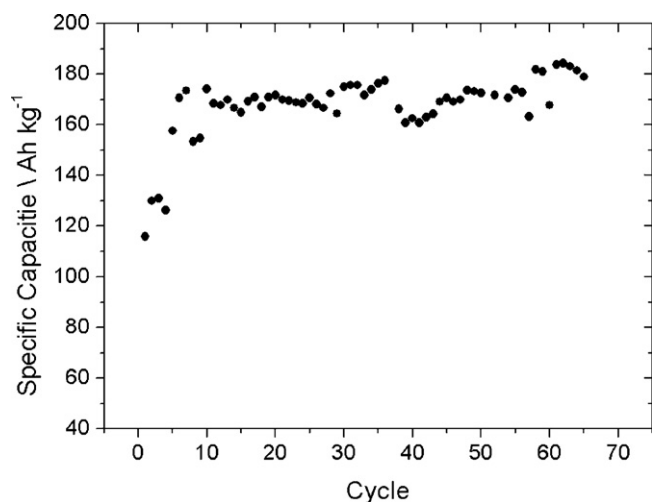


Fig. 11. Evolution of the specific capacity for a nanometric PbO_2 tubular electrode with a 3 mm diameter spine during pulsed charge cycles.

ization on the grid/PAM interface) and increase the amount of PAM participating in the discharge process.

4. Conclusions

It has been shown that it is possible to assemble a tubular electrode for lead acid batteries directly using chemically synthesised nanometric PbO_2 particle. Using a specific method to build up the connections among the particles and between the particles and the spine, it was possible to obtain electrodes with 180 Ah kg^{-1} that endured more than 130 cycles.

Despite the large surface area, the electrodes with nanometric PbO_2 were found to be highly resistive, as inferred from the high current pulsed charge experiments. The main component of the electrode global resistance was found to be the active material zone adjacent to the spine. This assessment was based on two observations: (1) the high overpotential during the pulsed charge

increased the conductivity of the PAM/spine interface and the PAM utilisation coefficient and (2) a decrease in the γ factor increased the PAM utilisation coefficient. Electrodes with specific capacities as high as 198 Ah kg^{-1} were successfully constructed.

Further work regarding the morphology of the PAM/spine interface is necessary.

Acknowledgements

Financial support of Paranaense Energy Company – COPEL. Laboratory Structure of Institute of Technology for Development – LACTEC.

TEM analysis: Ms. Rosângela Borges Freitas, from Electronic Microscopy Center of UFPR.

BET analysis: MSc. Orlando Baron.

References

- [1] D. Pavlov, J. Power Sources 33 (1991) 221.
- [2] D. Pavlov, E. Bashtavelova, J. Electrochem. Soc. 133 (1986) 241.
- [3] D. Pavlov, A. Dakhouche, T. Rogachev, J. Power Sources 42 (1993) 71.
- [4] M. Bervas, M. Perrin, S. Geniès, F. Mattera, J. Power Sources 173 (2007) 570.
- [5] D. Pavlov, J. Power Sources 53 (1995) 9.
- [6] G. Papazov, D. Pavlov, J. Power Sources 62 (1996) 193.
- [7] D. Pavlov, G. Papazov, B. Mohanov, J. Power Sources 113 (2003) 255.
- [8] P. Faber, in: D.H. Collins (Ed.), Power Sources 4, Oriel Press, Newcastle-upon-Tyne, 1973, pp. 525–538.
- [9] A. Caballero, M. Cruz, L. Hernán, J. Morales, L. Sánchez, J. Power Sources 113 (2003) 376.
- [10] A. Winsel, E. Voss, U. Hullmeine, J. Power Sources 30 (1990) 209.
- [11] Powder diffraction file JCPDS 35-1422.
- [12] B.D. Cullity, Elements of X-ray Diffraction, Addison Wesley, Massachusetts, 1956, p. 99.
- [13] J. de Andrade, R.V. Palmer, P.R. Impinnisi, Química Nova 34 (2011) 106.
- [14] C.V. D'Alkaine, P.R. Impinnisi, A. Carubelli, J. Power Sources 113 (2003) 293.
- [15] P.R. Impinnisi, C.V. D'Alkaine, J. de Andrade, J. Power Sources 85 (2000) 131.
- [16] D. Benchetrite, M. Le Gall, O. Bach, M. Perrin, F. Mattera, J. Power Sources 144 (2005) 346.
- [17] A. Kirchev, M. Perrin, E. Lemaire, F. Karoui, F. Mattera, J. Power Sources 177 (2008) 217.
- [18] H. Höpfinger, H. Winsel, J. Power Sources 55 (1995) 143.
- [19] A.F. Hollekamp, K.K. Constanti, M.J. Koop, L. Apateanu, M. Calabek, K. Micka, J. Power Sources 48 (1994) 195.